Original article

^{18}F Sodium Fluoride PET/CT in Patients with Prostate Cancer: Quantification of Normal Tissues, Benign Degenerative Lesions, and Malignant Lesions

Jorge D. Oldan, A. Stewart Hawkins, Bennett B. Chin

Department of Radiology, Division of Nuclear Medicine, Duke University Medical Center, Durham, North Carolina, USA

Abstract

Understanding the range and variability of normal, benign degenerative, and malignant ^{18}F sodium fluoride (^{18}F NaF) positron emission tomography/computed tomography (PET/CT) uptake is important in influencing clinical interpretation. Further, it is essential for the development of realistic semiautomated quantification techniques and simulation models. The purpose of this study is to determine the range of these values in a clinically relevant patient population with prostate cancer. ^{18}F NaF PET/CT scans were analyzed in patients with prostate cancer (n = 47) referred for evaluation of bone metastases. Mean and maximum standardized uptake values [SUVs (SUV_{mean} and SUV_{max})] were made in normal background regions (n = 470) including soft tissues (liver, aorta, bladder, adipose, brain, and paraspinal muscle) and osseous structures (T12 vertebral body, femoral diaphyseal cortex, femoral head medullary space, and ribs). Degenerative joint disease (DJD; n = 281) and bone metastases (n = 159) were identified and quantified by an experienced reader using all scan information including coregistered CT. For normal bone regions, the highest ^{18}F NaF PET SUV_{mean} occurred in T12 (6.8 ± 1.4) and it also showed the lowest coefficient of variation (cv = 21%). For normal soft tissues, paraspinal muscles showed very low SUV_{mean} (0.70 ± 0.11) and also showed the lowest variability (cv = 16%). Average SUV_{mean} in metastatic lesions is higher than uptake in benign degenerative lesions but values showed a wide variance and overlapping values (16.3 ± 13 vs 11.1 ± 3.8; P < 0.00001). The normal ^{18}F NaF PET uptake values for prostate cancer patients in normal background, benign degenerative disease, and osseous metastases are comparable to those reported for a general population with a wide variety of diagnoses. These normal ranges, specifically for prostate cancer patients, will aid in clinical interpretation and also help to establish the basis of normal limits in a semiautomated data analysis algorithm.

Keywords: Metastatic disease, normal value, positron emission tomography/computed tomography, prostate cancer, quantification, sodium fluoride

Introduction

^{18}F sodium fluoride (^{18}F NaF) positron emission tomography/computed tomography (PET/CT) is currently approved under the Centers for Medicare and Medicaid Services (CMS) designation of coverage under evidence development for the evaluation of bone metastases. It has demonstrated higher sensitivity and specificity compared to 99mTc-methylene diphosphonate (99mTc-MDP) planar and single-photon emission computed tomography (SPECT) imaging in detecting skeletal metastatic disease.[1,2] In patients with prostate cancer, it exhibits superior image quality compared to 99mTc-MDP bone scintigraphy, and better defines the extent of skeletal metastatic disease when compared to both conventional planar 99mTc-MDP bone scintigraphy and ^{18}F fluorodeoxyglucose (FDG) PET/CT.[3,4] It is both sensitive and specific for the detection of lytic and sclerotic malignant lesions and can accurately differentiate malignant from benign bone lesions.[5] A recent study demonstrated the ability of quantitative ^{18}F NaF PET/CT to delineate treatment response in patients with castration resistant prostate cancer (CRPC) bone metastases, and furthermore,

Access this article online

Quick Response Code:

Website: www.wjnm.org

DOI: 10.4103/1450-1147.172301

Address for correspondence:
Dr. Bennett B. Chin, Department of Radiology, Division of Nuclear Medicine, DUMC, Box 3808, Durham - 27710, North Carolina, USA.
E-mail: chin0004@dm.duke.edu

showed borderline correlation with progression free survival.[6] In addition to improved accuracy, ^{18}F NaF PET/CT has a significant impact in patient care, changing medical management in approximately 40% of patients.[7,8]

Despite the numerous benefits of ^{18}F NaF PET/CT, clinical interpretation and quantification often pose challenges. These challenges are frequently secondary to the overlap of ^{18}F NaF activity seen in both benign processes and metastatic disease. Establishing a set of reference uptake values for normal bone, benign skeletal processes, and metastatic disease could help diminish these challenges, serve to aid in clinical interpretation, and provide extremely valuable information to develop efficient and accurate semiautomated quantification algorithms. For FDG PET, the normal ranges have been previously reported;[9] however, only a single study has reported normal ^{18}F NaF PET/CT standardized uptake values (SUVs) in a population that included a wide variety of conditions.[10] To our knowledge, there are no reports for normal uptake, benign bone lesions, and malignant bone lesions specifically in patients with prostate cancer.

Currently, there is no accepted, standardized method available to quantify ^{18}F NaF PET/CT abnormalities. Despite this, novel ways to model normal and pathologic ^{18}F NaF PET/CT uptake are currently being investigated,[11] and ^{18}F NaF PET/CT is being used to evaluate response to novel therapies in prostate cancer.[6] The purpose of this study is to establish the range of SUV in normal, benign degenerative, and malignant lesions in a clinically relevant patient population in an effort to further develop semiautomated quantification models.

Materials and Methods

Study and patients

This study was reviewed and approved by our Institutional Review Board. The population included 47 male patients with prostate cancer referred for ^{18}F NaF PET/CT to evaluate for bone metastases. All patients had a peripheral intravenous catheter placed and verified for patency prior to administration of ^{18}F NaF (377.4 ± 13.7 MBq). The average uptake time was 65.7 ± 10.6 min (range 57-107; Table 1). All patients were instructed to void prior to imaging.

^{18}F NaF PET/CT image acquisition and reconstruction

All studies were performed on the same PET/CT scanner (GE Discovery 690, time-of-flight, 64-slice CT) with helical CT acquisition using either a nondiagnostic protocol (n = 40; noise index 35, 10-300 Smart mA, 140 kVp, thickness of 3.75 mm, 0.984 pitch ratio, rotation time 0.4 s) or a diagnostic protocol with IV contrast (n = 15; noise index 18, 50-750 Smart mA protocol, 120 kVp, 150 mL of Isovue injected at 3 cc/s, same table speed, and rotation). PET was performed via three-dimension (3-D) acquisition from the top of the skull to below the knees with the arms placed above the head, requiring 11-12 bed positions with a scan time of 2 min per 7.5-cm bed position. An iterative reconstruction was performed with OSEM using 2 iterations, 16 subsets, and a postreconstruction 6.4 mm Gaussian filter. All cases utilized time of flight reconstructions with CT attenuation correction and PET corrections for photon scatter, random events, and dead time.

Table 1: Demographics include age, weight, administered dose, and uptake time before scanning

Variable	Average (mean)	Standard deviation	Minimum	Maximum
Age (years)	69.4	7.9	48	82
Weight (kg)	90.9	15.9	60	128
Dose (MBq)	373.7	1.41	325.6	395.9
Time (min)	65.7	10.6	57	107

Image analysis

PET images were coregistered with CT images after acquisition using a commercial fusion viewer (MIMfusion, MIMvista, Cleveland, OH). A circular region of interest (ROI) was placed on six consecutive transaxial slices, with a size of 3 cm for liver, brain, adipose, bladder, and T12 areas. In cases with sufficient filling of the urinary bladder, the ROI for the urinary bladder was increased to 4.5 cm. Otherwise an ROI of 3 cm was used for the bladder. A 1.5-cm ROI was used for the aortic blood pool at the level of the aortic arch. A 7-mm ROI was used for the femoral cortex and ribs, as 7 mm was small enough to remain entirely within the area of interest. The lateral aspect of either the right or left sixth rib was used, except where metastases made it impossible to ascertain a normal value; in this case, the closest adjacent rib was used. Mean and maximum SUVs (SUV_{mean} and SUV_{max}, respectively) were recorded for each ROI.

Lesion classification and boundary definition

All of the available image information, including the coregistered CT, was utilized to classify all of the lesions as either benign degenerative or malignant. A board certified radiologist with expertise in nuclear medicine performed all classifications. Degenerative arthritic uptake characteristics included uptake centered on or adjacent to a joint, uptake corresponding to sclerosis at a joint, uptake in endplates of vertebral bodies or within osteophytes, or CT morphology generally suggestive of degenerative change. Malignant uptake characteristics

included uptake within trabecular marrow or a pattern and distribution of uptake typical for metastases such as uptake corresponding to classic CT findings such a round sclerotic lesion and focal uptake in the absence of a traumatic fracture. Equivocal lesions were omitted.

In contrast to a traditional absolute SUV contour threshold of 2.5 typically used in 18F FDG PET/CT research, the relatively high normal osseous background activity in NaF PET/CT images made it inappropriate to set an absolute contour threshold.[12-16] Instead, lesion boundaries were determined with a contour threshold of 50% of maximum SUV, similar to recent reports using thresholds of 40-50%.[17-19] All SUVs reported are from the time-of-flight reconstructions that were corrected for body weight.

Statistical analysis

The mean, standard deviation, range of values, and coefficients of variation (COV) were calculated for both the SUV_{mean} and SUV_{max}. A two-tailed *T*-Test (t = 0.05) was computed to compare group means such as the average SUV_{mean} of degenerative lesions compared to metastatic lesions. Additionally, SUVs from 10 different normal anatomic regions were correlated to patient's age, weight, and uptake time by calculating individual correlation coefficients. To account for multiple comparisons, a conservative significance level of P = 0.00167 was chosen based on utilizing a P value of 0.05 and 10 measurements for each of the three variables (30 measurements total; 0.05/30 = 0.00167). This calculation of correlation coefficients was performed for both SUV_{mean} and SUV_{max}.

Results

Individual SUV_{mean} and SUV_{max} measurements for normal, benign degenerative, and malignant lesions are shown in Table 2. As expected, osseous metastatic disease had the highest SUV_{mean} and SUV_{max}, with the exception of excreted activity in the urinary bladder. Soft tissues had very low retention of NaF activity, and no region, apart from bone and urine in the bladder, showed higher uptake compared to blood pool [Table 2]. The lowest coefficient of variation for SUV_{mean} and SUV_{max} was seen for the paraspinal muscles, but low values were also seen in the aorta and T12 vertebral body. Correlations coefficients between the SUV_{mean} of each anatomic region with age, weight, and uptake time showed a significant negative correlation between the T12 vertebral body and age (P = 0.0006), but no correlation with weight or uptake time. These same comparisons tested using SUV_{max} showed no statistically significant correlation.

The aortic blood pool and paraspinal muscles showed relatively low coefficients of variability. These regions were utilized as reference areas of normalization when computing normal osseous to background activity ratios [Table 3]. The ratios of normal osseous to background activity also showed a high variability. The ratio of lowest variability regions showed a mean SUV_{mean} T12/paravertebral ratio of approximately 10 with a coefficient of variation of 24%.

The SUV measurements of degenerative and metastatic disease varied widely. Average SUV_{mean} in metastatic lesions is higher than uptake in benign degenerative lesions, but there was significant overlap and the difference was not statistically significant (16.3 ± 13 vs 11.1 ± 3.8; P = 1.97). A lesion with a SUV_{mean} >30 was more commonly metastatic, although metastases could not be distinguished from degenerative disease or normal bone by SUV measurements alone. There was significant overlap of SUV_{mean} and SUV_{max} measurements from normal T12 vertebrae, degenerative disease, and metastatic disease [Table 2]. SUV_{mean} and SUV_{max} measurements for degenerative disease and

Table 2: SUV_{mean} and SUV_{max} of various regions

Region	Average (mean)		Standard deviation		Minimum		Maximum		Coefficient of variation	
	SUV_{Mean}	SUV_{Max}	SUV_{Mean}	SUV_{Max}	SUV_{Mean}	SUV_{Max}	SUV_{Mean}	SUV_{Max}	SUV_{Mean}	SUV_{Max}
Bladder	41.9	58.48	24.1	37.69	13.2	16.06	114.8	146.37	0.58	0.64
Liver	0.49	0.84	0.13	0.23	0.24	0.42	0.83	1.61	0.27	0.28
Aorta	1.21	1.61	0.24	0.33	0.65	0.97	1.71	2.26	0.20	0.21
Fat	0.18	0.41	0.05	0.14	0.11	0.22	0.32	0.81	0.28	0.33
Brain	0.15	0.34	0.04	0.12	0.02	0.18	0.22	0.70	0.26	0.34
Para. muscles	0.70	1.32	0.11	0.35	0.44	0.89	1.01	2.67	0.16	0.27
T12 Vertebra	6.80	9.32	1.44	1.82	4.19	6.29	11.58	15.72	0.21	0.20
Fem. Cortex	1.68	2.21	0.65	0.89	0.85	1.20	3.38	4.68	0.39	0.40
Femoral head	2.31	3.53	0.95	1.55	0.68	1.04	4.86	7.50	0.41	0.44
Rib	3.46	4.38	0.81	1.05	2.07	2.29	5.16	7.06	0.23	0.24
Degenerative	11.07	16.65	3.81	5.66	3.47	5.28	31.93	47.34	0.34	0.34
Metastatic	16.29	23.95	12.99	18.87	3.10	4.43	68.41	105.71	0.80	0.79

Average and range of SUV_{mean} and SUV_{max} values for normal regions, benign degenerative disease, and metastatic lesions

metastatic disease in different regions are presented in Table 4. Representative examples of ^{18}F NaF activity in degenerative lesions and osseous metastases are given in Figures 1-3.

Discussion

Using a combined PET/CT system, we quantified the normal bone, benign degenerative, and metastatic uptake by ^{18}F NaF PET/CT bone scan in a clinically relevant prostate cancer population. This population is particularly relevant because over 90% of patient with prostate cancer metastases have disease primarily involving the bone, and the majority of these patients have metastatic disease that may not be FDG avid.[20] Our results show a relatively wide range of values within each group, and significant overlap of SUVs between the groups. Despite the overlap, establishing a range of typical uptake values for various anatomic regions, benign osseous processes, and malignant osseous processes helps to guide clinical interpretation. It is also essential in establishing the foundation of semiautomated data analysis algorithms. The relatively high variability between patients in the normal structures suggest that a pre- and postmeasurement change of SUV_{mean} or SUV_{max} uptake within the patient[6] could be a much more sensitive means to assess response to therapy, rather than use of an absolute threshold or ratio.

A patient-specific model to help facilitate multicenter PET imaging protocols and analysis developed by Wilson *et al*. required segmentation of the CT portion of the NaF PET into various densities including soft tissue, air, bone cortex, and medullary bone.[11] Development of the model required absolute SUVs, derived from measurements in actual clinical patients. This model and other algorithms for semiautomated data analysis require realistic reference standards that may have significant variability between patients. In clinical FDG PET/CT, the liver SUV has shown relatively constant reproducibility despite variable uptake times ranging 1-3 h.[21] With ^{18}F NaF PET, however, the background uptake activity in the liver is both very low and shows relatively high variability. In work, using a canine model, time activity curves for NaF PET uptake in blood pool, liver, and bone were reported. These results showed a relatively wide range of SUV activity at 1 h; (liver 0.2 ± 0.2; ascending aorta 0.5 ± 0.1; humeral head 12.7 ± 2.6; T2 vertebral body 8.4 ± 0.9). Similar to NaF PET/CT time activity curves in patients,[22] the canine study showed a rapid drop in liver and blood pool activity, a modest drop in skeletal muscle activity, and a rapid increase in bone activity over 2 h of imaging.[23] Using liver activity 1 h after injection as a reference standard for ^{18}F NaF PET imaging would likely result in a wide range of values. While using blood pool activity 1 h after injection may have similar limitations, two recent studies investigated NaF activity in coronary and femoral arteries, respectively, by normalizing the activity in the arteries to background blood pool activity in the vena cava. In our attempts to measure activity in the vena cava, the cava was frequently surrounded by the liver, decompressed, or close to a calcified abdominal aorta. We, therefore, acquired blood pool activity measurements with a 1.5-cm ROI at the widest portion of the aortic arch, avoiding atherosclerotic calcification when present. Although our blood pool measurements

Table 3: SUV_{mean} and SUV_{max} bone/background ratios

Ratio	Average (mean)		Standard deviation		Minimum		Maximum		Coefficient of variation	
	SUV_{Mean}	SUV_{Max}	SUV_{Mean}	SUV_{Max}	SUV_{Mean}	SUV_{Max}	SUV_{Mean}	SUV_{Max}	SUV_{Mean}	SUV_{Max}
T12/paraspinal	9.71	7.06	2.39	2.54	5.43	3.33	15.34	19.04	0.24	0.34
Cortex/paraspinal	2.40	1.67	0.95	0.75	1.36	0.75	6.77	4.33	0.40	0.43
Fem head/paraspinal	3.30	2.67	1.39	1.25	0.95	0.97	6.37	5.65	0.42	0.45
Rib/paraspinal	4.94	3.31	1.26	1.07	3.05	1.48	7.67	7.34	0.26	0.31
T12/aorta	5.62	5.79	1.88	1.70	3.13	2.80	11.35	10.59	0.31	0.29
Cortex/aorta	1.39	1.37	0.58	0.60	0.64	0.58	3.83	4.25	0.40	0.43
Fem head/aorta	1.91	2.19	0.94	1.01	0.44	0.49	4.45	5.19	0.47	0.45
Rib/aorta	2.86	2.72	0.96	0.80	1.63	1.47	6.19	4.67	0.32	0.29

Ratios of bone to background activity SUV_{mean} and SUV_{max} values. Mean, standard deviation, minimum, maximum, and coefficient of variation (COV) are reported

Table 4: SUV_{mean} and SUV_{max} of osseous lesions

Region	Average (mean)		Standard deviation		Minimum		Maximum	
	SUV_{Mean}	SUV_{Max}	SUV_{Mean}	SUV_{Max}	SUV_{Mean}	SUV_{Max}	SUV_{Mean}	SUV_{Max}
Degenerative	11.07	16.65	3.81	5.66	3.47	5.28	31.93	47.34
All metastases	16.29	23.95	12.99	18.87	3.1	4.43	68.41	105.71
All nonrib metastases	18.21	26.89	13.70	20.04	4.2	6.34	68.41	105.71
Rib metastases	11.06	16.17	7.63	10.60	3.1	4.43	39.11	55.68
Spine metastases	23.13	34.24	16.21	24.2	8.86	13.01	68.41	105.71

SUV_{mean} and SUV_{max} measurements for degenerative disease, all metastases, all nonrib metastases, rib metastases, and spine metastases

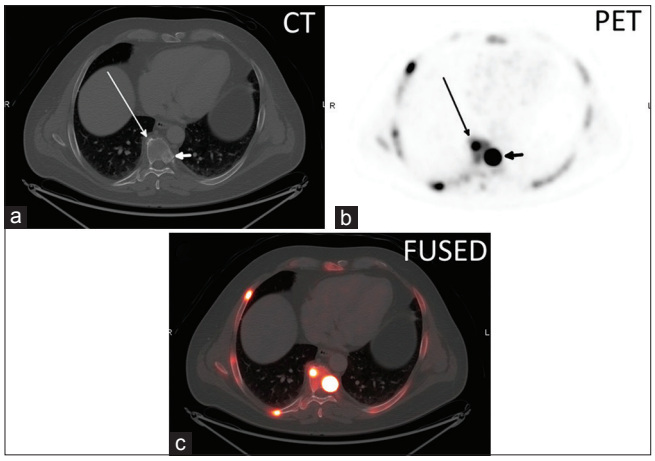

Figure 1: (a) Axial CT, (b) axial 18F NaF PET, and (c) axial fused PET/CT image of thoracic spine degenerative disc osteophyte (long arrow) with a SUV_{max} of 29.6 and an adjacent sclerotic vertebral body metastasis (short arrow) with a SUV_{max} of 95.6

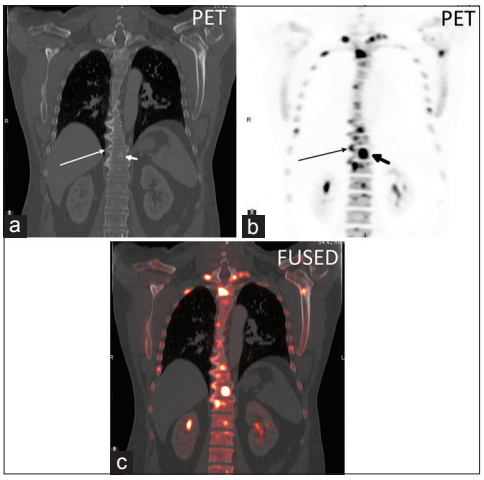

Figure 2: (a) Coronal CT, (b) coronal 18F NaF PET, and (c) axial fused PET/CT image in a thoracic spine degenerative disc osteophyte (long arrow) with a SUV_{max} of 27.3 and an adjacent sclerotic vertebral body metastasis (short arrow) with a SUV_{max} of 64.0

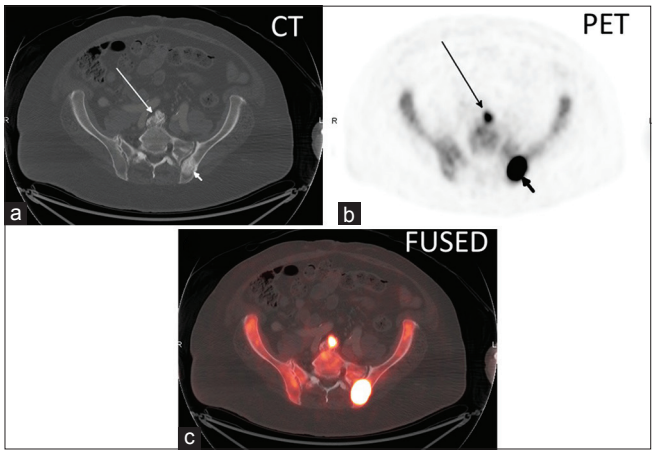

Figure 3: (a) Axial CT, (b) axial 18F NaF PET, and (c) axial fused PET/CT image in a lumbar spine degenerative disc osteophyte (long arrow) with a SUV_{max} of 20.7 and in a left posterior iliac bone sclerotic metastasis (short arrow) with a SUV_{max} of 101.5

had very low activity with a relatively high variability at an uptake time of 1 h, our measurements of ^{18}F NaF activity (SUV_{max} of 1.6) were in the range of previously reported values.[24,25]

We chose our various anatomic background regions based on the ease of measurement and potential for low variability. Paravertebral psoas muscle could serve as an easily measurable background region when evaluating the spine, a common site of prostate cancer metastases. Similarly, adipose tissue could provide a convenient background activity that could be measured on almost any axial slice, and brain uptake could be readily measured when evaluating the calvarium. Urine activity within the bladder was measured to potentially serve as an internal reference for the highest activity.

Among areas of normal background bone, we chose regions commonly affected by metastases in prostate cancer and attempted to include examples of both trabecular and cortical bone. The spine, femoral head, and ribs have a relatively large percentage of trabecular bone, whereas the distal femoral cortex has wide, continuous areas of cortical bone. We found a large amount of variability in ^{18}F NaF PET uptake in these different bone types. For instance, the mid-shaft femoral cortical bone showed overall lower uptake compared to osseous structures comprised primarily of trabecular bone, such as the T12 vertebral body. Attempts to quantify the pelvis were not successful due to variability in uptake due to its complex curves and variable thickness, particularly within the axial plane of imaging.

In our attempts to identify the best region to use for background normalization, the lowest coefficient of variation for background soft tissue and bone were within the paraspinal muscles and T12 vertebral body, respectively. The T12 vertebral body had a much higher uptake than the paraspinal muscles, and also a much higher range and standard deviation (average $SUV_{mean} = 6.80 \pm 1.44$). This uptake and variation compared reasonably well to prior reports of thoracic spine uptake by Sabbah *et al*. ($SUV_{mean} = 7.11 \pm 1.58$) and by Brenner *et al*. ($SUV_{mean} = 5.9 \pm 1.0$).[10,26] Our relatively high standard deviation was present despite a relatively uniform patient population of prostate cancer patients and a narrow uptake imaging time window compared to a prior report that included an unselected patient population and a broader uptake time window of 139 min.[10] In addition, we report a relatively wide range of ^{18}F NaF PET activity in normal bone, which is important to consider when interpreting metastatic lesions. For example, to maintain sufficient image contrast for metastatic lesion detection, the upper threshold for SUV should be higher than that of normal bone, commonly as high as SUV of 10 when evaluating the spine.

We calculated the normal ratio of T12 uptake to paraspinal muscle uptake (bone/background) in order to determine the range of normal bone to muscle uptake ratio, analogous to the relatively consistent background liver uptake in FDG PET.[21] While the T12/paraspinal muscle ratio for SUV_{mean} showed a lowest coefficient of variation of all of the bones to background combinations calculated, there was still a relatively wide range in the calculated ratios (5.43-15.34).

In addition to determining the best internal reference standard to apply normalization, understanding how uptake time changes target and background measurements is critical in applying the semiautomated quantification algorithm. Earlier work with ^{18}F NaF PET explored the kinetic relationship of plasma NaF concentration and skeletal NaF uptake, using subjects with normal bone or patients with osteoporotic bone. Neither of the studies focused on patients with osseous metastatic disease.[27,28] The earlier noted canine model showed that ^{18}F NaF activity in bone increases rapidly and then continues to increase gradually for hours, while activity in blood pool and solid organs declines rapidly in the first 20 min, with minimal decrease in activity thereafter.[23] Recently, ^{18}F NaF SUV time activity curves for human subjects with normal bone and in patients with metastatic skeletal disease have been published.[22] These curves showed a similar gradual increase of ^{18}F NaF activity in the bone and a gradual decrease in ^{18}F NaF blood pool activity over time.[22] From all of these studies, it can be concluded that target to background calculations will depend greatly on uptake time. With our relatively narrow uptake time range of 57-107 min, our correlation coefficients did not show an effect of uptake time on SUV_{mean} or SUV_{max} measurements.

The data from our study and those from a recent work by Sabbah *et al*. followed the Society of Nuclear Medicine (SNM) practice guideline. ^{18}F NaF PET/CT bone scans 1.0.[10,29] There is good agreement between our SUV measurements and their reported measurements for blood pool activity, soft tissue, normal bone, degenerative change, and metastatic disease. One advantage of our study was that all of our patients were scanned on the same PET/CT scanner rather than two different machines. Additionally, the range of uptake time for our patients was smaller (57-107 min vs 30-169 min). Nevertheless, data from our measurements, Sabbah *et al*., and Nagarajah *et al*. indicate that there is a relatively high variability in background SUV activity in bone and soft tissues.[10,30]

This retrospective study has a number of limitations. First, all patients were prostate cancer patients which makes this relevant for most patients, but it does not define the values for true normal controls. This population, however, has a very high incidence of bone metastases, and may be the most clinically relevant population from which a reference range of ^{18}F NaF PET/CT scans can be derived for comparison. Second, the clinical information is incomplete, and thus, the prognostic value and the clinical and histopathologic confirmation are not available. These results rely upon the interpretation by an experienced reader who is capable of integrating imaging characteristics (location, configuration, distribution, and CT findings) to determine the proper classification. This study, however, reports a realistic clinical scenario in which SUV measurements are performed. Lastly, our calculation of correlation coefficients did show a negative correlation between patient age and SUV_{mean} of T12. One hypothesis is that this could reflect an age-related decrease in bone remodeling within the spine due to demineralization. Additional prospective studies of normal patients, including females, would be helpful in determining the normal ^{18}F NaF uptake and variability. Further studies correlating clinical parameters and histopathology with imaging findings would also be useful for interpretation.

Conclusion

The normal ^{18}F NaF PET uptake within background soft tissue, bone, benign degenerative disease, and osseous metastases specifically measured in prostate cancer patients are very similar to those reported for a general population. Normal soft tissues have a very low normal uptake, with the lowest variability measured in the paravertebral muscles. The highest normal bone uptake was measured at T12; this region also had the lowest normal variability. These normal ranges, specifically for prostate cancer patients, will aid in clinical interpretation and also help to establish the basis of normal limits in a semiautomated data analysis algorithm.

References

1. Even-Sapir E, Metser U, Mishani E, Lievshitz G, Lerman H, Leibovitch I. The detection of bone metastases in patients with high-risk prostate cancer: 99mTc-MDP planar bone scintigraphy, single- and multi-field-of-view SPECT, 18f-fluoride PET, and 18F-fluoride PET/CT. J Nucl Med 2006;47:287-97.
2. Tateishi U, Morita S, Taguri M, Shizukuishi K, Minamimoto R, Kawaguchi M, *et al*. A meta-analysis of (18) F-Fluoride positron emission tomography for assessment of metastatic bone tumor. Ann Nucl Med 2010;24:523-31.
3. Cook GJ, Fogelman I. The role of positron emission tomography in skeletal disease. Semin Nucl Med 2001;31:50-61.
4. Iagaru A, Mittra E, Dick DW, Gambhir SS. Prospective evaluation of (99m) Tc MDP scintigraphy, (18) F NaF PET/CT, and (18) F FDG PET/CT for detection of skeletal metastases. Mol Imaging Biol 2012;14:252-9.
5. Even-Sapir E, Metser U, Flusser G, Zuriel L, Kollender Y, Lerman H, *et al*. Assessment of malignant skeletal disease: Initial experience with 18F-fluoride PET/CT and comparison

between 18F-fluoride PET and 18F-fluoride PET/CT. J Nucl Med 2004;45:272-8.

6. Yu EY, Duan F, Muzi M, Deng X, Chin BB, Alumkal JJ, *et al*. Castration-resistant prostate cancer bone metastasis response measured by 18F-fluoride PET after treatment with dasatinib and correlation with progression-free survival: Results from American College of Radiology imaging network 6687. J Nucl Med 2015;56:354-60.
7. Hillner BE, Siegel BA, Hanna L, Duan F, Quinn B, Shields AF. 18F-fluoride PET used for treatment monitoring of systemic cancer therapy: Results from the national oncologic PET registry. J Nucl Med 2015;56:222-8.
8. Hillner BE, Siegel BA, Hanna L, Duan F, Shields AF, Coleman RE. Impact of 18F-fluoride PET in patients with known prostate cancer: Initial results from the national oncologic PET registry. J Nucl Med 2014;55:574-81.
9. Wang Y, Chiu E, Rosenberg J, Gambhir SS. Standardized uptake value atlas: Characterization of physiological 2-deoxy-2-[18F] fluoro-d-glucose uptake in normal tissues. Mol Imaging Biol 2007;9:83-90.
10. Sabbah N, Jackson T, Mosci C, Jamali M, Minamimoto R, Quon A, *et al*. 18F-sodium fluoride PET/CT in oncology: An atlas of SUVs. Clin Nucl Med 2014;40:e228-31.
11. Wilson JM, Chisholm KL, Oldan JD, Segars P, Turkington TG, Chin BB. Patient-specific model of NaF PET to facilitate multicenter clinical trial PET imaging protocols and analysis: Preliminary results of a CT-based simulation. J Nucl Med 2013;54(Suppl 1):3A-35.
12. Hyun SH, Ahn HK, Kim H, Ahn MJ, Park K, Ahn YC, *et al*. Volume-based assessment by (18) F-FDG PET/CT predicts survival in patients with stage III non-small-cell lung cancer. Eur J Nucl Med Mol Imaging 2014;41:50-8.
13. Kim DH, Son SH, Kim CY, Hong CM, Oh JR, Song BI, *et al*. Prediction for recurrence using F-18 FDG PET/CT in pathologic N0 lung adenocarcinoma after curative surgery. Ann Surg Oncol 2014;21:589-96.
14. Patz EF Jr, Lowe VJ, Hoffman JM, Paine SS, Burrowes P, Coleman RE, *et al*. Focal pulmonary abnormalities: Evaluation with F-18 fluorodeoxyglucose PET scanning. Radiology 1993;188:487-90.
15. Satoh Y, Onishi H, Nambu A, Araki T. Volume-based parameters measured by using FDG PET/CT in patients with stage I NSCLC treated with stereotactic body radiation therapy: Prognostic value. Radiology 2014;270:275-81.
16. Lowe VJ, Fletcher JW, Gobar L, Lawson M, Kirchner P, Valk P, *et al*. Prospective investigation of positron emission tomography in lung nodules. J Clin Oncol 1998;16:1075-84.
17. Usmanij EA, de Geus-Oei LF, Troost EG, Peters-Bax L, van der Heijden EH, Kaanders JH, *et al*. 18F-FDG PET early response evaluation of locally advanced non-small cell lung cancer treated with concomitant chemoradiotherapy. J Nucl Med 2013;54:1528-34.
18. Akkas BE, Demirel BB, Dizman A, Vural GU. Do clinical characteristics and metabolic markers detected on positron emission tomography/computerized tomography associate with persistent disease in patients with in-operable cervical cancer? Ann Nucl Med 2013;27:756-63.
19. Melloni G, Gajate AM, Sestini S, Gallivanone F, Bandiera A, Landoni C, *et al*. New positron emission tomography derived parameters as predictive factors for recurrence in resected stage I non-small cell lung cancer. Eur J Surg Oncol 2013;39:1254-61.
20. Jadvar H. Prostate cancer: PET with 18F-FDG, 18F- or 11C-acetate, and 18F- or 11C-choline. J Nucl Med 2011;52:81-9.
21. Chin BB, Green ED, Turkington TG, Hawk TC, Coleman RE. Increasing uptake time in FDG-PET: Standardized uptake values in normal tissues at 1 versus 3 h. Mol Imaging Biol 2009;11:118-22.
22. Kurdziel KA, Shih JH, Apolo AB, Lindenberg L, Mena E, McKinney YY, *et al*. The kinetics and reproducibility of 18F-sodium fluoride for oncology using current PET camera technology. J Nucl Med 2012;53:1175-84.
23. Valdes-Martinez A, Kraft SL, Brundage CM, Arceneaux BK, Stewart JA, Gibbons DS. Assessment of blood pool, soft tissue, and skeletal uptake of sodium fluoride F 18 with positron emission tomography-computed tomography in four clinically normal dogs. Am J Vet Res 2012;73:1589-95.
24. Dweck MR, Chow MW, Joshi NV, Williams MC, Jones C, Fletcher AM, *et al*. Coronary arterial 18F-sodium fluoride uptake: A novel marker of plaque biology. J Am Coll Cardiol 2012;59:1539-48.
25. Janssen T, Bannas P, Herrmann J, Veldhoen S, Busch JD, Treszl A, *et al*. Association of linear ^{18}F-sodium fluoride accumulation in femoral arteries as a measure of diffuse calcification with cardiovascular risk factors: A PET/CT study. J Nucl Cardiol 2013;20:569-77.
26. Brenner W, Vernon C, Muzi M, Mankoff DA, Link JM, Conrad EU, *et al*. Comparison of different quantitative approaches to 18F-fluoride PET scans. J Nucl Med 2004;45:1493-500.
27. Hawkins RA, Choi Y, Huang SC, Hoh CK, Dahlbom M, Schiepers C, *et al*. Evaluation of the skeletal kinetics of fluorine-18-fluoride ion with PET. J Nucl Med 1992;33:633-42.
28. Cook GJ, Lodge MA, Blake GM, Marsden PK, Fogelman I. Differences in skeletal kinetics between vertebral and humeral bone measured by 18f-fluoride positron emission tomography in postmenopausal women. J Bone Miner Res 2000;15:763-9.
29. Segall G, Delbeke D, Stabin MG, Even-Sapir E, Fair J, Sajdak R, *et al*.; SNM. SNM practice guideline for sodium 18F-fluoride PET/CT bone scans 1.0. J Nucl Med 2010;51:1813-20.
30. Nagarajah J, Dannat T, Hartung V, Bockisch A, Rosenbaum-Krumme S. 18F-fluoride PET/CT for bone scanning. Role of attenuation correction. Nuklearmedizin 2012;51:84-7.

How to cite this article: Oldan JD, Hawkins AS, Chin BB. ^{18}F sodium fluoride PET/CT in patients with prostate cancer: Quantification of normal tissues, benign degenerative lesions, and malignant lesions. World J Nucl Med 2016;15:102-8.

Source of Support: Nil. **Conflict of Interest:** None declared.